Journal of Optimization in Industrial Engineering
Vol.15, Issue 2, Summer & Autumn 2022, 179- 190
Doi: 10.22094/joie.2022.1932748.1868

Research Article

Reliability Analysis of a Mounted Moldboard Plow Bottom Standard Using the FORM Method

Seyed Mohammad Reza Nazemosadat [a], Mojtaba Naderi-Boldaji [a,*], Davoud Ghanbarian [b], Mohammad Amin Nematollahi [c]

[a]*Department of Mechanical Engineering of Biosystems, Faculty of Agriculture, Shahrekord University, Shahrekord, 88186-34141, Iran*
[b]*Department of Industrial Design, Faculty of Applied Arts, University of Art, Tehran, 1136813518, Iran*
[c]*Department of Biosystems Engineering, Faculty of Agriculture, Shiraz University, Shiraz, Iran*

Received **08** June 2021; Revised 14 April 2022; Accepted 17 April 2022

Abstract

Using the reliability index to express a system's safety, reliability theory is applied to study a structure's failure probability due to the uncertainty (i.e., randomness) of design and production parameters with (a) variability in working conditions and the environment and (b) direct interaction with the soil, the conventional approach has been based on deterministic design methods. In contrast, using the concept of reliability as a new and useful approach, we develop the industry of design and manufacture of agricultural machinery. In this study, the first-order reliability method (FORM) was used to analyze the reliability of a plow bottom standard. To perform the reliability analysis, the required forces on the standard were determined by simulating the interaction of the plow with the soil using finite element method by Abaqus software. Random variables were considered as longitudinal and vertical forces on the bottom standard, radius of the standard arc, plastic cross-section modulus, and yield stress. The reliability index (β) as a measure of the system's safety of was determined using reliability analysis whose value was found to be 2.569 for the bottom's standard. Moreover, the failure probability (Pf) of the bottom's standard was calculated as 0.005. In the final step, the results of FORM reliability analysis were compared with the reliability results of the Monte Carlo simulation of the plow bottom's standard. The results showed that the bottom standard's probability of failure in the FORM and Monte Carlo methods for the conditions considered—i.e., very compacted soil, plowing depth of 30 cm, and velocity of 3 m s-1—are low and almost low, respectively. Also due to the lack of lateral force FX in the limit state function, the FORM analysis indicated sufficient uncertainty of the bottom standard design; therefore, strengthening or optimizing this part of the moldboard plow chassis seems necessary.

***Keywords*:** Reliability; FORM method; Moldboard plow; Standard; Finite element.

1. Introduction

Structural reliability is a scale by which the ability of any part of a structure or an entire structure can be measured under the conditions for which it is intended (Lee et al., 2002). To express a system's safety, the *reliability index* is used as a tool to measure reliability and to some extent avoid the problem of risky numerical values (Kaveh and Kalat jari, 1994).

Development of appropriate methods for reliability analysis and designs' optimization has been the focus of many studies in the field of engineering in recent decade (e.g., Saidi-Mehrabad and Fazlollahtabar, 2016; Sharifi and Yaghoubizadeh, 2015). In engineering problems, a series of uncertainties vary according to the nature of the problem and the method of analysis. In designing and constructing structures, engineers face various types of uncertainties, including physical uncertainty, model uncertainty, and statistical uncertainty. Because of the statistical nature of the loads on the structure, reliability cannot be considered a definite variable. Accordingly, we face a statistical problem with various uncertainties; therefore, analyzing the reliability of structures is important (Keshtegar et al., 2011).

Types of uncertainty in the amount of load applied, geometry, and properties of materials can be considered through probabilistic analysis of structural and mechanical components (Keshtegar, 2018). The main effort in the first-order reliability analysis is to calculate the reliability index based on the minimum distance between the failure level and the source in the standard normal space (Hasofer and Lind, 1974; Elegbede, 2005), which can be similar to a relationship optimization problem (Keshtegar and Miri, 2014).

In engineering discussions, the issue of safety and failure is expressed in different ways such that the theory of reliability, considering uncertain quantities and random variables, considers these concepts as probabilities. In a system's analysis, the limit state between safety and failure is generally expressed by the function g(R,Q) in which Q and R represent the random variable of load and resistance, respectively (Ghohani Arab and Ghasemi, 2018). In this case, failure occurs when the load exceeds the resistance. According to this definition and from a structural perspective, when the structure's response

*Corresponding author Email address: naderi.mojtaba@sku.ac.ir

exceeds a similar resistance, failure occurs in the system (Nowak and Collins, 2000).

In recent decades, many efforts have been made to develop appropriate and practical methods for analyzing the reliability of structures. Among them, the first-order reliability method (FORM) and the second-order reliability method (SORM)—known as *analytical methods*—were introduced in 1974 by Hasofer and Lind to determine the reliability index (Hasofer and Lind, 1974). Due to the significant superiority of probabilistic analysis (compared to definitive analysis) in covering uncertainties, much research has recently been done on using the FORM (Shabakhti et al., 2021; Keshtegar, 2018; Moghimi, 2020; Dudzik, and Potrzeszcz-Sut, 2019).

Reliability of a structure is the structure's ability to complete and satisfy design goals for a specified design period, or useful life. Reliability is often identified with its complement, the possibility of failure—i.e., the possibility that a structure will not perform its expected function. The term *failure* does not necessarily mean catastrophic failure but is used to indicate that the structure does not function as described (Shayanfar et al., 2015).

Including reliability in designing agricultural machinery is also a new approach to overcome the drawbacks of the old (i.e., classic) design and achieve an optimal and more reliable design (Kharmnda et al., 2014). Although the probabilistic design approach has been widely used in many industrial fields, none of these approaches have been considered in designing tillage machines (Abo Al-Kheer et al., 2011).

For the first time, a design approach based on reliability in tillage machines was developed by Abo Al-Kheer et al. (2011). For this purpose, two validation methods—i.e., the Monte Carlo simulation method and the first-order reliability method (FORM)—were used. This approach was implemented to design the standard of a chisel plow. The results showed that the standard has a high degree of reliability. However, in order to achieve the best design solution from an economic viewpoint, minimizing the volume of the chisel plow standard structure with a design approach based on reliability was considered. In another study, design optimization based on a chisel plow's standard reliability optimization was determined using Kharmnda et al.'s (2011) Optimal Safety Coefficient (OSF) strategy. The OSF approach was extended to several nonlinear probability distributions, such as the lognormal, uniform, Weibull, and Gumbel probability distribution rules. The probability density function (PDF) of the horizontal force on the chisel plow standard was also obtained. The results revealed that the reliability-based design could lead to trustworthy and low cost structures.

The moldboard plow is one of the oldest and most important tillage implements. From 2002 to 2017, the number of moldboard plows in Iran increased from 230,000 to about 350,000, indicating that conventional tillage employed the moldboard plow is widely used in Iran (Agricultural Statistics, 2002-2017). According to these statistics, the use of the moldboard plow has increased in recent years despite recommendations for protecting soil resources.

Tillage machines and tools directly interact with the soil in such a way that the parameters and variables affecting their design are inherently random. Therefore, \reliability concepts can be used as a suitable approach in designing and constructing tillage machines and tools.

This study's purpose was to analyze the reliability of the mounted moldboard plow bottom standards. One of the most important parts of the plow structure, the plow bottom's standard is affected by the soil's variable and random forces by moving the plow in the field and performing tillage operations. If the standard requirements are not considered in designing and constructing the bottom's standard, this part of the plow structure will fail, resulting in the tillage operation's disruption.

A literature review shows that (a) few scientific studies on design and analysis are based on the reliability of the plow chassis and (b) domestic manufacturers usually build on the basis of empirical information. In this study's first stage, plow modeling is done by using SOLIDWORKS 2016 software. After transferring the model to Abaqus 2018 software, the finite plow-soil components are analyzed; and the forces acting on the plow are extracted from the soil. In the second stage, the reliability analysis of the plow bottom's standard is performed using the first-order reliability (FORM) method (in this analysis, the F_Z and F_Y forces extracted from the finite element analysis are also considered part of the random variables). Hasofer and Lind's FORM reliability analysis method is used to calculate and analyze the reliability index (β) and the probability of failure (P_f) of the moldboard plow bottom's standard. In the last step, the results of the plow bottom's standard reliability analysis using the FORM are compared with the results of the plow bottom's standard reliability analysis using the Monte Carlo simulation method.

2. Materials and Methods

Fig. 1 shows the three-bottom reversible mounted moldboard plow (P12-3, GAK Co., Mashhad, Iran) simulated in this study.

Fig. 1. The three-bottom mounted moldboard plow used in this study.

After identifying the plow's details and dimensions and modeling the actual geometry, the plow was modeled in SOLIDWORKS 2016 software. Fig. 2 shows the various parts and views of the three-dimensional plow model.

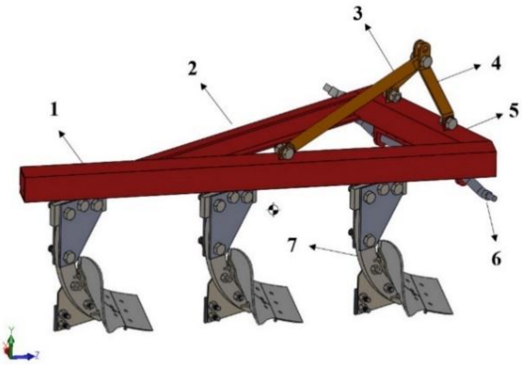

Fig. 2. 3D model of moldboard plow in SOLIDWORKS 2016 software: (1) longitudinal toolbar, (2)side toolbar, (3) brace, (4) mast, (5) lateral toolbar,(6) cross bar, (7) bottom standard.

Fig. 3 shows a 3D model of plow-soil interaction using Abaqus software. In this model, the soil box with 3.5 m × 2.5 m × 1 m (i.e., length × width × height) was modeled. To identify the forces acting on the plow structure, the moldboard plow was analyzed as a rigid body. The *soil's mechanical behavior* was also defined as the elastic-perfectly plastic with linear Drucker-Prager yield criteria (Nazemosadat et al., 2022). After the forces acting on the plow in different soil conditions were estimated, the plow components of CK45 and ST52 steel were defined in the chassis static analysis in which the structure was viewed as deformable.

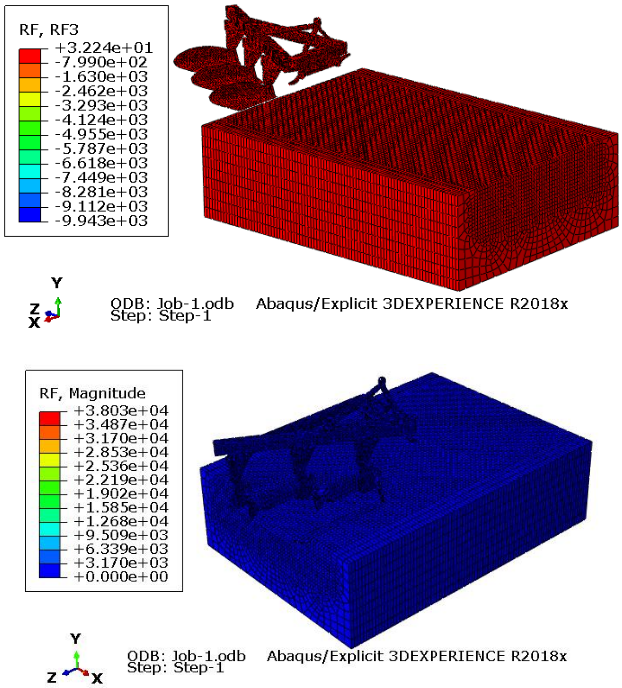

Fig. 3. Finite element analysis of soil's reaction force on a plow at a plowing depth of d = 30 cm.

For meshing the moldboard plow and soil, C3D10 (i.e., 10-node tetrahedral element) and C3D8R (i.e., 8-node linear brick continuum elements), respectively, were used (Nazemosadat et al., 2022).

In the analysis of plow-soil interaction, longitudinal (F_Z), lateral (F_X), and vertical (F_Y) forces on the plow in the most critical state (depth of 0.30 m and velocity of 3 m s^{-1}) with very compacted soil properties were determined. In static analysis, according to the forces extracted from the plow-soil interaction analysis and its application on the plow, the stress applied on different parts of the plow chassis was analyzed.

2.1. First-Order reliability method (FORM)

In 1969, using the first moment (mathematical expectation) and the second moment (covariance) to express the stochastic variables' properties and the linearization of the limit condition function using the Taylor expansion, Cornell presented the reliability index as the following:

$$\beta = \frac{\mu_g}{\sigma_g} \tag{1}$$

where $\boldsymbol{\mu_g}$ is the mean and $\boldsymbol{\sigma_g}$ is the standard deviation of the function g. Based on Fig. 4, the Cornell reliability index—as a measured distance from the mean of the g function to the failure level—provides a good estimate of the reliability. The failure level indicates the boundary between the safety zone ($\boldsymbol{g(R,Q) > 0}$) and the failure zone ($\boldsymbol{g(R,Q) < 0}$). According to Fig. 4, this distance is measured as a multiple of the parameter$\boldsymbol{\sigma_g}$.

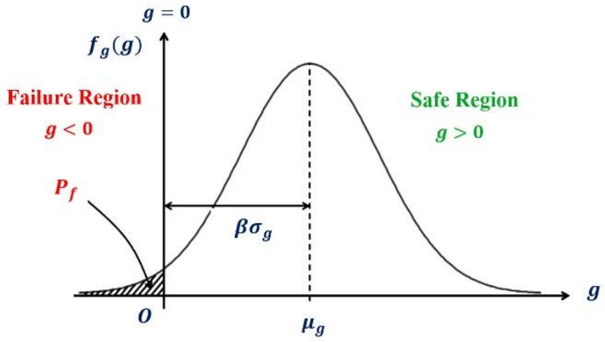

Fig. 4. Cornell's reliability index parameters.

If the design variables have a normal distribution function and the failure level is a super-plane, Eq. 1 provides an accurate estimate of the reliability and failure probability index. When the failure level is not super-planed, the reliability index can be calculated using Eq. 2 by linearizing the g function and using the first-order Taylor expansion:

$$\beta = g(\mu_{u1}, \mu_{u2}, \dots, \mu_{un}) \Bigg/ \sqrt{\sum_{i=1}^{n} \left(\frac{\partial g}{\partial U_i} . \sigma_{Ui} \right)^2} \tag{2}$$

where U is the standard variable in the reduced normal space. Thus, the probability of failure can be calculated with the help of the reliability index calculated as $P_f = \Phi(-\beta)$ in which Φ is a function of variable cumulative distribution with standard normal distribution (Nowak and Collins, 2000).

2.2. Problem definition

As mentioned in the introduction, the plow bottom standard is one of the parts of the plow structure that is affected by the soil's variable and random forces during tillage operations. Therefore, the bottom standard, which is one of the most important parts of the plow structure, which is likely to break during work (especially in critical conditions). For this reason, the reliability of the plow bottom standard and ultimately its optimization must be analyzed.

Analytical methods using mathematical formulas and solutions to express a problem and its solutions are based on finding the most probable point of failure (MPPF), which is also called the *design point* (Fig. 5). In these methods, a criterion is first defined as a *reliability index* or *safety index* and denoted by β. This index represents the distance from the coordinates' origin to the level corresponding to the limit state function in the random variables' standardized space (i.e., space u_1-u_2). Two well-known analytical methods are the first-order reliability method (FORM) and the second-order reliability method (SORM). The FORM method (Fig. 5), introduced by Hasofer and Lind (1974) and used in this paper, is based on the fact that the failure function is in practice usually a nonlinear function. Therefore, to simplify the problem, the failure function's linear approximation is used at the design point and in the standard normal space.

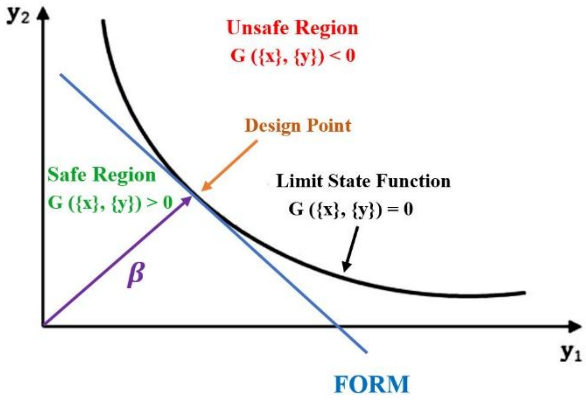

Fig. 5. Procedure image of First-Order Reliability Method (FORM).

The reliability relationship is defined based on two important parameters: strength and load on the structure. The failure probability function is written as the following (Nowak and Collins, 2000):

$$g(R, Q) = R - Q \tag{3}$$

Where $\boldsymbol{g(R,Q)}$ is the limit state function of structure's load and resistance. In Eq. 3, each of the two functions of resistance (R) and load (Q) consists of several random variables with different probability distribution functions that depend on the dimensions' nature, the type of structural materials, and the loads applied. The *area of structural failure* is defined based on the limit state function (g), according to the relationship between resistance and load; therefore, the structure's failure probability is calculated as follows (Nowak and Collins, 2000):

$$P_f = P[\mathrm{g(R - Q)} \leq 0] = \int_{\mathrm{g(R-Q)} \leq 0} \mathrm{f_X}(X) d_X \tag{4}$$

This integral represents the area of the probability distribution function of the base random variables ($\boldsymbol{f_X(X)}$) to the failure limit$\boldsymbol{R - Q \leq 0}$, indicating the structure's failure probability (P_f), which is the opposite of the reliability index (***β***). The higher reliability index (***β***) results in a lower probability of failure (P_f).

In analyzing the reliability of the plow bottom's standard due to the randomness of soil properties' parameters, the soil's forces applied on the plow bottom are also considered random variables. These forces include the vertical force applied to the bottom (F_y) and the tensile strength applied to the bottom (F_z), which are calculated by simulating the plow-soil interaction in Abacus. The radius of the arc of the standard (R) also changes in size due to the variable tensile strength (F_z); therefore, this variable is considered random. The plastic cross-section modulus (Z) and yield stress (σ_y), which are the characteristics of the bottom standard, are the bottom standard's random parameters due to the variable forces applied to the standard. The plastic cross-section modulus (Z) is calculated as follows:

$$Z = (S.F) \times S \ , \quad S = \frac{I}{C} \tag{5}$$

where the parameters I, C, S, and S.F are the moment of bending inertia, the distance from neutral axis, the elastic section module, and the cross-sectional shape factor, respectively.

2.3. Reliability analysis of moldboard plow bottom standards using the FORM analytical method

In this study, the following steps were performed to analyze the reliability of the standard of a moldboard plow bottom using the FORM analytical method.

2.3.1. Determining random variables

Stochastic variables for reliability analysis by FORM method included vertical force on the bottom (F_y), longitudinal force on the bottom (F_z), standard arch radius (R), plastic cross-sectional modulus (Z), and yield stress (σ_y). To calculate the random variables of vertical force on the bottom (F_y) and of longitudinal force applied on the bottom (F_z), plow-soil interaction was simulated in Abaqus software at the most critical depth of 30 cm and at the forward speed of 3 m s^{-1} with the soil very compacted.

2.3.2. Selecting the type of probability distribution for the random variable

To select the best distribution for the random variables, the data related to these variables were analyzed using EasyFit software. For this purpose, eight different distribution functions—the uniform distribution functions, frechet, exponential, beta, normal, lognormal, weibull and rayieigh—were selected for each random variable. After extracting the data distribution function and histogram, Chi-square comparison was used and the best probability distribution was selected and scored for each random variable. The Chi-square test was used to match the probability distribution function with the data frequency histogram. The following equation shows how this experiment works:

$$x^2 = \frac{\sum(n_i - e_i)^2}{e_i} \tag{6}$$

where x^2 is the error rate of each distribution function. Rank 1 would be assigned to the function that is the least different from the data histogram (Sorensen, 2004). In Fig.6, $\mathbf{n_i}$ and e_i represent the function value and observed value, respectively.

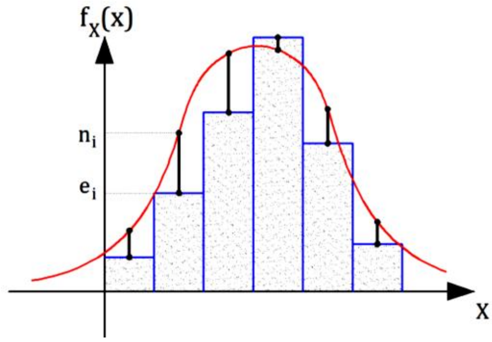

Fig. 6. Representation of n_i and e_i in the Chi-square test (Miar Naeimi et al., 2016).

According to studies conducted in relation to a structure's reliability analysis (Abo Al-kheer et al., 2011; Mojahed and Ahmdi Nedushan, 2013; Kharmnda et al., 2014), most of the normal and lognormal distributions are used as the best distributions. In the normal distribution, also known as the Gaussian distribution, the value of the probability density function (PDF) is obtained from the following:

$$f_x(x) = \frac{1}{\sigma\sqrt{2\pi}} exp\left[-\frac{1}{2}\left(\frac{x-\mu}{\sigma}\right)^2\right] \tag{7}$$

where x is the random variable, μ is the mean, and σ is the standard deviation.

In addition, in normal distribution the value of the cumulative distribution function (CDF) is equal to the following:

$$F(x) = \int_{-\infty}^{x} f_x(x)dx = \int_{-\infty}^{x} \frac{1}{\sigma\sqrt{2\pi}} \exp\left[-\frac{1}{2}\left(\frac{x-\mu}{\sigma}\right)^2\right]dx \tag{8}$$

If the variable x has a lognormal distribution with a mean of μ' and a standard deviation of σ',

$$\mu' = \exp(\mu + \frac{\sigma^2}{2}) \tag{9}$$

$$\sigma'^2 = (\exp\sigma^2 - 1)\exp(2\mu + \sigma^2) \tag{10}$$

In the lognormal distribution, the value of the probability density function (PDF) is obtained from the following:

$$f_x(x) = \frac{1}{x\sigma\sqrt{2\pi}} exp\left[-\frac{1}{2}\left(\frac{Lnx - \mu}{\sigma}\right)^2\right] \tag{11}$$

Furthermore, in this distribution the value of the cumulative distribution function (CDF) is equal to the following:

$$F(x) = \int_{-\infty}^{x} f_x(x)dx = \int_{-\infty}^{x} \frac{1}{x\sigma\sqrt{2\pi}} \exp\left[-\frac{1}{2}\left(\frac{Lnx-\mu}{\sigma}\right)^2\right]dx \tag{12}$$

2.3.3. Determining the limit state function

A comprehensive examination of the chassis types of moldboard plows produced domestically or imported shows that the standard's cross-sectional area is mostly rectangular plows; and as noted above, the standard with the mentioned section has a specified length in two shapes: arched or straight. In the moldboard plow selected for this study, the standard is arched, as shown in Fig. 7. The amount of torque applied to the arched standard on the YZ plane due to the forces ($\boldsymbol{F_y}$) and ($\boldsymbol{F_z}$) is equal to the following:

$$\boldsymbol{M = F_z.R(1-\cos\theta) - F_y.R.\sin\theta} \quad (13)$$

where M is the torque on the standard, $\boldsymbol{F_y}$ is the vertical force on the bottom standard, $\boldsymbol{F_z}$ is the longitudinal force on the bottom standard, and R is the radius of the standard arch. The limit state function for a moldboard plow bottom standard is defined as follows:

$$\boldsymbol{g(F_y, F_z, R, Z, \sigma_y) = Z\sigma_y - F_z.R(1-\cos\theta) + F_y.R.\sin\theta \le 0} \quad (14)$$

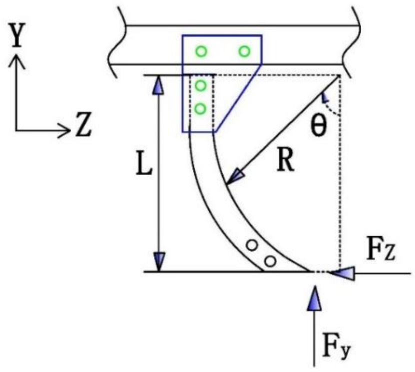

Fig. 7. Forces on the bottom's arched standard in the side view.

2.3.4. Calculating standard reliability index by using the FORM method

In this study, Hasofer and Lind's method was used to calculate the reliability index (β). In 1974, Hasofer and Lind proposed that the reliability index in nonlinear limit state functions for a particular problem would remain constant by changing the limit state function. Based on the Cornell idea and the reliability index, this method uses the linear form method of limit state function and first and second order constraints to obtain the answer (Hasofer and Lind, 1974). Instead of using the averaging point in calculating the reliability index, Hasofer and Lind used a new point called the *design point* (Fig. 8) in the standardized coordinate system (Sorensen, 2004; Nowak and Collins, 2000).

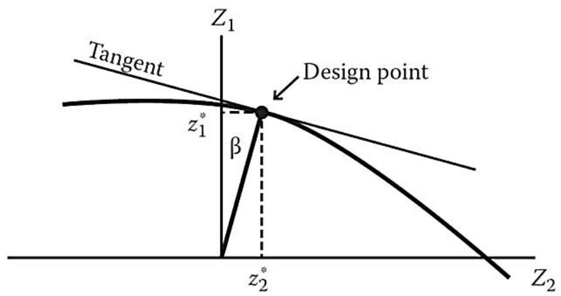

Fig. **8.** Hasofer and Lind's design points and reliability index (Nowak and Collins, 2012).

In this new design space, the geometric distance between the origin and the transmitted limit state function is defined as an indicator of reliability. To obtain the design point's coordinates including $\{\boldsymbol{Z_1^*, Z_2^*, \dots, Z_n^*}\}$ in the trial and error phase, it is necessary to solve the $\boldsymbol{2n+1}$ equation in which *n* is the number of random variables. These equations include the following: beta (β) equation, $\boldsymbol{n}$ equation $\boldsymbol{\alpha_i}$ equals the sensitivity coefficient, and $\boldsymbol{n}$ equation $\boldsymbol{Z_i^*}$ or design points (Sorensen, 2004; Nowak and Collins, 2000).

In Hasofer and Lind's method, the limit state function is evaluated at the MPPF)—i.e., the point on the limit state surface that has the highest probability of failure. Because MPPF is not known in advance, an iterative technique should be used to determine Hasofer and Lind's reliability index, which is considered a baseline with independent variables of resistance R and stress S that have normal distributions (Shayanfar et al., 2015). In Hasofer and Lind's method, in the first step, the standard normal random variables are expressed as follows (Sorensen, 2004; Nowak and Collins, 2000):

$$\boldsymbol{\hat{R} = \frac{R-\mu_R}{\sigma_R}}, \quad \boldsymbol{\hat{S} = \frac{S-\mu_s}{\sigma_s}} \quad (15)$$

In the next step, the limit state surface g (R, S) = R-S = 0 in the initial coordinate system (R, S) becomes the limit state surface in the standard normal coordinate system (Eq. 16) (Shayanfar et al., 2015):

$$\boldsymbol{g\left(R(\hat{R}), S(\hat{S})\right) = \hat{g}(\hat{R}, \hat{S}) = \hat{R}\sigma_R - \hat{S}\sigma_S + (\mu_R - \mu_S) = 0} \quad (16)$$

where the shortest distance from the center of the coordinate system $\boldsymbol{(\hat{R}, \hat{S})}$ to the rupture level $\boldsymbol{\hat{g}(\hat{R}, \hat{S}) = 0}$ is equal to the reliability index $\boldsymbol{\beta = \hat{O}P^* = (\mu_R - \mu_S)/\sqrt{\sigma_R^2 + \sigma_S^2}}$ is as shown in Fig. 9. According to Fig. 9, the point $\boldsymbol{P^*(\hat{R}^*, \hat{S}^*) = 0}$ in $\boldsymbol{\hat{g}(\hat{R}, \hat{S}) = 0}$, which is the shortest distance to the origin of the coordinate system. This point is known as the most probable failure point (MPPF).

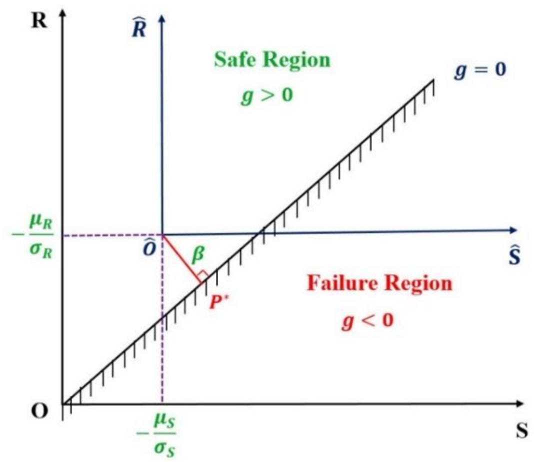

Fig. 9. Geometric interpretation of Hasofer and Lind's reliability index.

In Hasofer and Lind's method, the probability of failure is based on finding the minimum distance of a point on the limit condition function to the origin in standard normal space, which aims to find the most probable point based on the optimization model(Shayanfar et al., 2015):

$$\begin{aligned}&\boldsymbol{Minimize}:\ \boldsymbol{\beta}(\boldsymbol{U}) = (\boldsymbol{U}^{T}\boldsymbol{U})^{\frac{1}{2}}\\&\boldsymbol{Subject\ to}:\ \boldsymbol{g}(\boldsymbol{U}) = \boldsymbol{0}\end{aligned} \tag{17}$$

Where $\boldsymbol{\beta}$ is the reliability index and $\boldsymbol{g}(\boldsymbol{U})$ is the limit state function in standard normal space (Fig. 10). To solve the above optimal problem, the limit state function with $\boldsymbol{n}$ independent and normal random variables is considered as the following:

$$\boldsymbol{g}(\boldsymbol{X}) = \boldsymbol{g}(\{\boldsymbol{x_1}, \boldsymbol{x_2}, \dots, \boldsymbol{x_n}\}^{\boldsymbol{T}}) = \boldsymbol{0} \tag{18}$$

The principal variables of the limit state function $\boldsymbol{g}(\boldsymbol{X})$ become their standard form according to the following (Shayanfar et al., 2015):

$$\boldsymbol{u_i} = \frac{\boldsymbol{x_i} - \boldsymbol{\mu_{x_i}}}{\boldsymbol{\sigma_{x_i}}} \tag{19}$$

where $\boldsymbol{\mu_{x_i}}$ and $\boldsymbol{\sigma_{x_i}}$ are the mean value and standard deviation of the random variable $\boldsymbol{x_i}$, respectively, and $\boldsymbol{u_i}$ is the standard normal random variable.

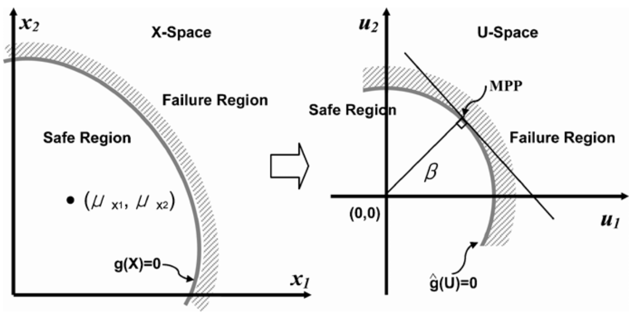

Fig. 10. Mapping the failure surface from space X to space U.

According to Fig. 10, the failure surface g (X) = 0 in space X is mapped to the corresponding failure surface g (U) = 0 in space U.

The limit state function g (X) can be linear or nonlinear. Based on the conversion given in Eq. 19, the limit state function of Eq. 18 is mapped as follows (Shayanfar et al., 2015):

$$\begin{aligned}\boldsymbol{g}(\boldsymbol{U}) = \boldsymbol{g}\Big(\{&\boldsymbol{\sigma_{x_1}u_1} + \boldsymbol{\mu_{x_1}}, \boldsymbol{\sigma_{x_2}u_2}\\&+ \boldsymbol{\mu_{x_2}}, \dots, \boldsymbol{\sigma_{x_n}u_n} + \boldsymbol{\mu_{x_n}}\}^{\boldsymbol{T}}\Big) = \boldsymbol{0}\end{aligned} \tag{20}$$

The first-order expansion of the Taylor series at the limit state function's MPPF point is expressed as follows (Shayanfar et al., 2015):

$$\widetilde{\boldsymbol{g}}(\boldsymbol{U}) \approx \boldsymbol{g}(\boldsymbol{U}^{*}) + \sum_{\boldsymbol{i}=\boldsymbol{1}}^{\boldsymbol{n}} \frac{\boldsymbol{\partial g}(\boldsymbol{U}^{*})}{\boldsymbol{\partial U_i}}(\boldsymbol{u_i} - \boldsymbol{u_i^{*}}) \tag{21}$$

Based on Eq. 19, we derive the following (Sorensen, 2004; Nowak and Collins, 2000; Shayanfar et al., 2015):

$$\frac{\boldsymbol{\partial}\widehat{\boldsymbol{g}}(\boldsymbol{U})}{\boldsymbol{\partial u_i}} = \frac{\boldsymbol{\partial g}(\boldsymbol{X})}{\boldsymbol{\partial x_i}}\boldsymbol{\sigma_{x_i}} \tag{22}$$

Therefore, the approximate value of the reliability index in each iteration cycle is equal to the following (Sorensen, 2004; Nowak and Collins, 2000; Shayanfar et al., 2015):

$$\widehat{\boldsymbol{O}}\boldsymbol{P}^{*} = \boldsymbol{\beta} = \frac{\boldsymbol{g}(\boldsymbol{U}^{*}) - \sum_{\boldsymbol{i}=\boldsymbol{1}}^{\boldsymbol{n}} \frac{\boldsymbol{\partial g}(\boldsymbol{U}^{*})}{\boldsymbol{\partial x_i}}\boldsymbol{\sigma_{x_i}u_i^{*}}}{\sqrt{\sum_{\boldsymbol{i}=\boldsymbol{1}}^{\boldsymbol{n}}\left(\frac{\boldsymbol{\partial g}(\boldsymbol{U}^{*})}{\boldsymbol{\partial x_i}}\boldsymbol{\sigma_{x_i}}\right)^{\boldsymbol{2}}}} \tag{23}$$

The direction cosine of the unit's external vertical vector is calculated as follows (Sorensen, 2004; Nowak and Collins, 2000; Shayanfar et al., 2015):

$$\cos\boldsymbol{\theta_{x_i}} = -\frac{\frac{\boldsymbol{\partial g}(\boldsymbol{X}^{*})}{\boldsymbol{\partial x_i}}\boldsymbol{\sigma_{x_i}}}{\left[\sum_{\boldsymbol{i}=\boldsymbol{1}}^{\boldsymbol{n}}\left(\frac{\boldsymbol{\partial g}(\boldsymbol{X}^{*})}{\boldsymbol{\partial x_i}}\boldsymbol{\sigma_{x_i}}\right)^{\boldsymbol{2}}\right]^{\boldsymbol{1/2}}} = \boldsymbol{\alpha_i} \tag{24}$$

Where $\boldsymbol{\alpha_i}$ represents a random variable's relative effect corresponding to the total change, which is called the *sensitivity coefficient*. The coordinates of point *P* are calculated as the following (Sorensen, 2004; Nowak and Collins, 2000; Shayanfar et al., 2015):

$$\boldsymbol{u_i^{*}} = \frac{\boldsymbol{x_i^{*}} - \boldsymbol{\mu_{x_i}}}{\boldsymbol{\sigma_{x_i}}} = \widehat{\boldsymbol{O}}\boldsymbol{P}^{*}\cos\boldsymbol{\theta_{x_i}} = \boldsymbol{\beta}\cos\boldsymbol{\theta_{x_i}} \tag{25}$$

The coordinates corresponding to the point *P* in the main space are in the form of Eq. 26 (Sorensen, 2004; Nowak and Collins, 2000; Shayanfar et al., 2015):

$$\boldsymbol{x_i^{*}} = \boldsymbol{\mu_{x_i}} + \boldsymbol{\beta\sigma_{x_i}}\cos\boldsymbol{\theta_{x_i}}, (\boldsymbol{i} = \boldsymbol{1}, \boldsymbol{2}, \dots, \boldsymbol{n}) \tag{26}$$

By transferring the new design points to the original coordinate system and repeating the mentioned steps to converge, the reliability index and design points are obtained. For example, some of the calculations performed in relation to the analysis of the bottom standard reliability from the FORM method in the first iteration to achieve convergence in subsequent iterations are the following:

$$\boldsymbol{g}(\boldsymbol{X_1}) = \boldsymbol{g}(\boldsymbol{F_y}, \boldsymbol{F_z}, \boldsymbol{R}, \boldsymbol{Z}, \boldsymbol{\sigma_y}) \tag{27}$$

$$\boldsymbol{\beta_1} = -\frac{g(X_1)}{\left[\left(\frac{\partial g(X_1)}{\partial F_y}\sigma_{F_y}\right)^2 + \left(\frac{\partial g(X_1)}{\partial F_z}\sigma_{F_z}\right)^2 + \left(\frac{\partial g(X_1)}{\partial R}\sigma_R\right)^2 + \left(\frac{\partial g(X_1)}{\partial Z}\sigma_Z\right)^2 + \left(\frac{\partial g(X_1)}{\partial(\sigma_y)}\sigma_{(\sigma_y)}\right)^2\right]^{1/2}} \tag{28}$$

$$\boldsymbol{\alpha_{F_y}} = -\frac{\frac{\partial g(X_1)}{\partial F_y}\sigma_{F_y}}{\left[\left(\frac{\partial g(X_1)}{\partial F_y}\sigma_{F_y}\right)^2 + \left(\frac{\partial g(X_1)}{\partial F_z}\sigma_{F_z}\right)^2 + \left(\frac{\partial g(X_1)}{\partial R}\sigma_R\right)^2 + \left(\frac{\partial g(X_1)}{\partial Z}\sigma_Z\right)^2 + \left(\frac{\partial g(X_1)}{\partial(\sigma_y)}\sigma_{(\sigma_y)}\right)^2\right]^{1/2}} \tag{29}$$

$$\boldsymbol{\alpha_{F_z}} = -\frac{\frac{\partial g(X_1)}{\partial F_z}\sigma_{F_z}}{\left[\left(\frac{\partial g(X_1)}{\partial F_y}\sigma_{F_y}\right)^2 + \left(\frac{\partial g(X_1)}{\partial F_z}\sigma_{F_z}\right)^2 + \left(\frac{\partial g(X_1)}{\partial R}\sigma_R\right)^2 + \left(\frac{\partial g(X_1)}{\partial Z}\sigma_Z\right)^2 + \left(\frac{\partial g(X_1)}{\partial(\sigma_y)}\sigma_{(\sigma_y)}\right)^2\right]^{1/2}} \tag{30}$$

$$\boldsymbol{\alpha_R} = -\frac{\frac{\partial g(X_1)}{\partial R}\sigma_R}{\left[\left(\frac{\partial g(X_1)}{\partial F_y}\sigma_{F_y}\right)^2 + \left(\frac{\partial g(X_1)}{\partial F_z}\sigma_{F_z}\right)^2 + \left(\frac{\partial g(X_1)}{\partial R}\sigma_R\right)^2 + \left(\frac{\partial g(X_1)}{\partial Z}\sigma_Z\right)^2 + \left(\frac{\partial g(X_1)}{\partial(\sigma_y)}\sigma_{(\sigma_y)}\right)^2\right]^{1/2}} \tag{31}$$

$$\boldsymbol{\alpha_Z} = -\frac{\frac{\partial g(X_1)}{\partial Z}\sigma_Z}{\left[\left(\frac{\partial g(X_1)}{\partial F_y}\sigma_{F_y}\right)^2 + \left(\frac{\partial g(X_1)}{\partial F_z}\sigma_{F_z}\right)^2 + \left(\frac{\partial g(X_1)}{\partial R}\sigma_R\right)^2 + \left(\frac{\partial g(X_1)}{\partial Z}\sigma_Z\right)^2 + \left(\frac{\partial g(X_1)}{\partial(\sigma_y)}\sigma_{(\sigma_y)}\right)^2\right]^{1/2}} \tag{32}$$

$$\boldsymbol{\alpha_{\sigma_y}} = -\frac{\frac{\partial g(X_1)}{\partial(\sigma_y)}\sigma_{(\sigma_y)}}{\left[\left(\frac{\partial g(X_1)}{\partial F_y}\sigma_{F_y}\right)^2 + \left(\frac{\partial g(X_1)}{\partial F_z}\sigma_{F_z}\right)^2 + \left(\frac{\partial g(X_1)}{\partial R}\sigma_R\right)^2 + \left(\frac{\partial g(X_1)}{\partial Z}\sigma_Z\right)^2 + \left(\frac{\partial g(X_1)}{\partial(\sigma_y)}\sigma_{(\sigma_y)}\right)^2\right]^{1/2}} \tag{33}$$

$$U_{F_y} = \frac{F_y-\mu_{F_y}}{\sigma_{F_y}} \quad , \quad U_{F_z} = \frac{F_z-\mu_{F_z}}{\sigma_{F_z}} \quad , \quad U_R = \frac{R-\mu_R}{\sigma_R} \quad , \quad U_Z = \frac{F_Z-\mu_Z}{\sigma_Z} \quad , \quad U_{\sigma_y} = \frac{\sigma_y-\mu_{\sigma_y}}{\sigma_{(\sigma_y)}} \tag{34}$$

Next, the reliability index is obtained using the FORM method by considering Eq. 14 as a limit state function for each of the soil forces. Also, the convergence of the reliability index (β) is calculated as the following (Sorensen, 2004; Nowak and Collins, 2000; Shayanfar et al., 2015):

$$\boldsymbol{\varepsilon} = \frac{|\boldsymbol{\beta_{i+1}} - \boldsymbol{\beta_i}|}{\boldsymbol{\beta_i}} \quad , \qquad \boldsymbol{i \geq 1} \tag{35}$$

3. Results and Discussion

3.1. FORM analysis

In this section, the FORM is applied to calculate the bottom's standard reliability index (β) and the probability of failure (P_f) (Subsection 3.1.3). To determine these parameters (β and P_f), the probability distribution (Subsection 3.1.1) as well as the probabilistic and statistical characteristics of each random variable (Subsection 3.1.2) must be found. The random variables are F_y, F_z, Z, R, and σ_y. In this problem, the random variables and two parameters (β and P_f) were considered as the input and output of the FORM analysis.

3.1.1. Random variables and probability distributions

Fig. 11 shows the results of the data analysis using EasyFit software to select the best probability distribution for the random variable of longitudinal force applied to the bottom ($\boldsymbol{F_z}$). The horizontal axis represents the amount of longitudinal force and the vertical axis indicates the frequency of data.

Eight distribution functions—uniform distribution functions, frechet, exponential, beta, normal, lognormal, weibull, and rayieigh—were selected for the random variable of longitudinal force on the bottom ($\boldsymbol{F_z}$) and were compared using the Chi-squared test. These functions were ranked from one to eight accordingly. The results revealed that Rank 1 is related to the normal probability distribution and Rank 8 is associated with the exponential distribution. Consequently, the normal probability distribution was designated as the best distribution for the random variable of longitudinal force on the bottom ($\boldsymbol{F_z}$).Likewise, Chi-square test was applied for other variables; and the best type of distribution was considered for other random variables, including the radius of the bottom's standard arc (R), plastic cross-sectional modulus (Z), and yield stress ($\boldsymbol{\sigma_y}$) of the normal distribution chassis.

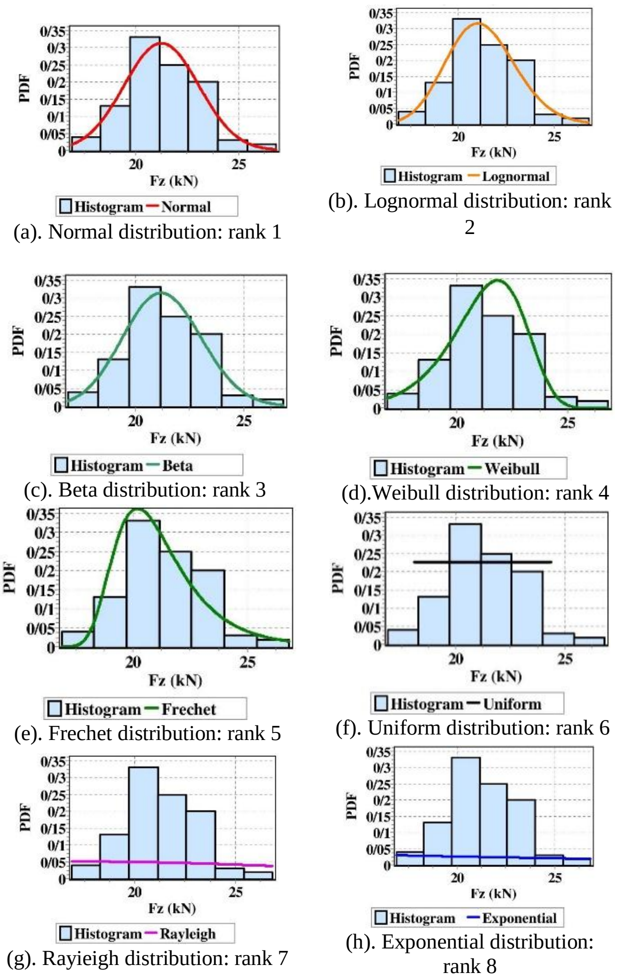

(a). Normal distribution: rank 1
(b). Lognormal distribution: rank 2
(c). Beta distribution: rank 3
(d).Weibull distribution: rank 4
(e). Frechet distribution: rank 5
(f). Uniform distribution: rank 6
(g). Rayieigh distribution: rank 7
(h). Exponential distribution: rank 8

Fig. 11. Probability functions calculated for longitudinal force on the bottom ($\boldsymbol{F_z}$) and their ranking.

3.1.2. *Probability and statistical characteristics of random variables*

Table 1 presents the randomly selected variables' probability characteristics related to the moldboard plow's standard. According to the selected normal probability distribution, the standard deviation and the mean of random variables were extracted.
Table 2 shows the statistical characteristics of random variables related to the moldboard plow's standard.

Table 1
Probability properties of the plow bottom's standard random variables.

Random variables	Unit	Type of distribution	Distribution parameters
Bottom standard arch radius, R	m	Normal	$\boldsymbol{\sigma = 0.0095}$, $\boldsymbol{\mu = 0.5398}$
Plastic cross-sectional modulus, Z	m^3	Normal	$\boldsymbol{\sigma = 1.99 \times 10^{-5}}$, $\boldsymbol{\mu = 7.636 \times 10^{-5}}$
Longitudinal force applied to the standard of each bottom, F_z	kN	Normal	$\boldsymbol{\sigma = 1.8178}$, $\boldsymbol{\mu = 21.262}$
Vertical force applied to the standard of each bottom, F_y	kN	Normal	$\boldsymbol{\sigma = 0.3162}$, $\boldsymbol{\mu = 2.248}$
Yield stress, σ_y	MPa	Normal	$\boldsymbol{\sigma = 33769}$, $\boldsymbol{\mu = 4.165 \times 10^{5}}$

Table 2
Statistical characteristics of the plow bottom's standard random' variables.

Random variables	mean	Variance	Range	Coefficient of variation
Bottom standard arch radius, R	0.539	9.03×10^{-5}	0.0425	0.176
Plastic cross-sectional modulus, Z	7.63×10^{-5}	3.96×10^{-10}	1.10×10^{-4}	0.260
Longitudinal force applied to the standard of each bottom, F_z	21.262	3.304	9.969	0.085
Vertical force applied to the standard of each bottom, F_y	2.248	0.099	1.543	0.140
Yield stress, σ_y	4.16×10^{5}	1.14×10^{9}	1.69×10^{5}	0.081

3.1.3. *Calculation of failure probability (P_f) and reliability index (β)*

After extracting the random variables according to the limit state function's value considered for the moldboard plow bottom standard, the value of reliability index (β) was calculated in three repetitions up to convergence (Table 3). Also, the probability of failure (P_f) was calculated according to the relationship $P_f = \Phi(-\beta)$. As shown in Table 3, the values of the reliability index (β) and failure probability (P_f) were calculated as equal to 2.568 and 0.005, respectively, after reaching the convergence, thus indicating a low failure probability for the bottom standard given the defined conditions. As shown in Table 3, the sensitivity coefficients (α_k) also indicate that the random variable of plastic cross-sectional modulus (Z) has the greatest effect on the bottom standard's probability of failure (P_f).

Table 3
The result of the iterations in the FORM reliability analysis for the moldboard plow bottom standard.

Iteration No.	1	2	3
$g(F_y, F_z, R, Z, \sigma_y)$	22.719	1.134	-0.0517
$\dfrac{\partial g(X_k)}{\partial F_y}$	0.5400	0.54019	0.54037
$\dfrac{\partial g(X_k)}{\partial F_z}$	-0.5400	-0.54019	-0.54037
$\dfrac{\partial g(X_k)}{\partial R}$	-15.4260	-19.5326	-19.6098
$\dfrac{\partial g(X_k)}{\partial Z}$	414×10^{3}	391×10^{3}	405×10^{3}
$\dfrac{\partial g(X_k)}{\partial \sigma_y}$	75×10^{-6}	29.8×10^{-6}	26×10^{-6}
β	2.496975	2.56938	2.56887
P_f	0.006483	0.005201	0.005212
α_{F_y}	-0.01929	-0.02154	-0.02088
α_{F_z}	0.11090	0.12383	0.12008

α_R	0.01655	0.02340	0.02277
α_Z	-0.93551	-0.98363	-0.98645
α_{σ_y}	-0.29111	-0.12697	-0.10736
F_{y_k}	2.8840	2.2327	2.2304
F_{z_k}	18.3100	21.7653	21.8403
R_k	0.5400	0.54019	0.54037
Z_k	75×10^{-6}	29.8×10^{-6}	26×10^{-6}
σ_{y_k}	414×10^{3}	391×10^{3}	405×10^{3}
u_{F_y}, k	2.0113	-0.0483	-0.05537
u_{F_z}, k	-1.6223	0.2768	0.31817
u_R, k	0.0210	0.0410	0.06010
u_Z, k	-0.06532	-2.3358	-2.52733
u_{σ_y}, k	-0.0740	-0.7269	-0.32633
ε	-	0.02899	0.000197

3.2. Monte Carlo simulation

The reliability analysis of the moldboard plow bottom standard was also performed using the Monte Carlo simulation method, one of the random simulation methods for structural reliability analysis. In stochastic simulation methods, the reliability indices are estimated based on the actual process simulation according to the system's random behavior. Therefore, in these methods, the problem is simulated in the form of a number of experiments similar to real-time experiences. In fact, the Monte Carlo method is a computational algorithm using random sampling to calculate the results.

Fig. 12 shows the Monte Carlo simulation's results of the bottom standard in terms of standard stress and yield stress. In this diagram, the green, gray, and red circles represent the areas of, safety, limit state function, and failure, respectively.

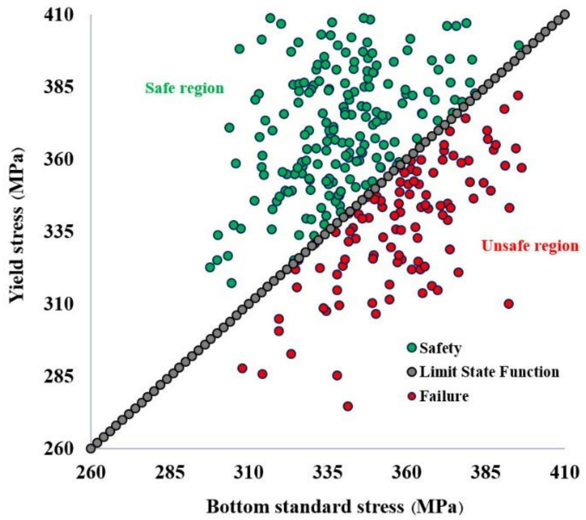

Fig. 12. The Monte Carlo simulation's results in terms of bottom standard stress and yield stress.

According to Fig. 12, considering that the number of stress variables in the safety area (green circles) is more than the number of stress variables in the failure area (red circles), it can be concluded that the probability of failure for bottom standard is almost low.

Based on Table 4, after simulation process implementation in Abaqus and the extraction of Von-Mises stress (σ_y) variables—according to the value of the limit state function $g(\mathrm{x}) = \sigma_y - \sigma_{max}$ and the amount of yield stress on the bottom standard—the plow bottom standard's failure probability (P_f) was calculated.

Table 4
The probability of failure (P_f) and reliability index (β) of bottom standard in different Monte Carlo simulations.

Name of the part		Number of simulations		
		100	200	300
standard	P_f	310×10^{-3}	304×10^{-3}	296×10^{-3}
	β	0.5566	0.5742	0.5976

A comparison of the results of the FORM (Table 3) and the Monte Carlo (Table 4) analyses of the bottom standard shows that the bottom standard's probability of failure for the applied conditions (i.e., very compacted soil, plow depth of 30 cm, and plow speed of 3 m s^{-1}) is low and almost low, respectively. It is noted that one of the differences in the reliability index's value between the FORM and Monte Carlo methods is that the force F_x is not considered in the FORM method.

4. Conclusions

This study's purpose the reliability of the moldboard plow bottom standard. The FORM analysis method was used to analyze the reliability. The analysis showed that the bottom standard has moderate reliability considering the longitudinal (F_z) and vertical forces (F_y). Because of (a) the limited application of lateral force (F_x) on the bottom standard in the FORM analytical method and (b) the fact that this force is not considered in the limit state function, it is predicted that with the bottom standard resulting from applying all three force components, its reliability index decreases. Thus, the bottom's standard must be strengthened in more critical conditions. Moreover, the comparison of the random variables' sensitivity coefficients (α_k) showed that the random variable of the plastic cross-section module (Z) has the greatest effect on the bottom standard's probability of failure (P_f) and that the random variables of vertical force (F_y) and standard radius (R) have the least effect on the magnitude of the bottom standard's probability of failure (P_f). (See Table 3.)

Acknowledgment

Dr. Farzaneh Khorsandi, Department of Biological and Agricultural Engineering, University of California at Davis, USA is thanked for her help in proof readings of the revised manuscript.

Conflict of Interest

The authors declared no potential conflicts of interest rega rding this paper's research, authorship, and publication.

Funding

The authors received no financial support for the research, authorship, and publication of this article.

Nomenclature

Symbols	
d	Plowing depth (cm)
E_s	Soil Young' modulus (kPa)
E_m	Moldboard Young's modulus (kPa)
$\boldsymbol{e_i}$	Observed value
$\boldsymbol{F}(\mathbf{x})$	Cumulative distribution function
F_z	Draft (longitudinal) force per bottom body (kN)
F_x	Lateral force per bottom body (kN)
F_v	Vertical force per bottom body (kN)
$\boldsymbol{F_R}(\boldsymbol{Q})$	The function of the cumulative distribution of the system resistance
$\boldsymbol{f_x}(\boldsymbol{x})$	Probability density function
$\boldsymbol{g}(\boldsymbol{R},\boldsymbol{Q}), \boldsymbol{g}(\mathbf{x})$	Limit state function
$\boldsymbol{g}(\boldsymbol{U})$	Limit state function in standard normal space
M	Torque (kN.m)
$\boldsymbol{N_F}$	Number of structural failure times
N	Number of repetitions
$\boldsymbol{n_i}$	Value of the function
P_f	Probability of failure
Q	Load
$\boldsymbol{Q_i}$	Load on the i element (part)
$\widehat{\boldsymbol{R}}$	Resistance
R	Bottom standard arch radius (m)
$\boldsymbol{R_i}$	Resistance of the i element (part)
v	Plowing speed (m s^{-1})
Z	Plastic cross-sectional modulus (m^3)
$\boldsymbol{\sigma_g}$	Standard deviation of the limit state function
$\boldsymbol{\sigma_Q}$	Standard deviation of the load function
$\boldsymbol{\sigma_R}$	Standard deviation of the resistance function
$\boldsymbol{\sigma_y}$	Yield stress (kPa)
σ_v	Von-Mises stress
σ	Standard deviation (in normal distribution)
$\boldsymbol{\sigma_{x_i}}$	Standard deviation of the random variable x_i
σ'	Standard deviation (in lognormal distribution)
$\boldsymbol{\sigma_{max}}$	Maximum Von-Mises stress
σ_c	Compressive yield stress (kPa)
ρ	Density (g cm^{-3})
$\boldsymbol{\rho_{RQ}}$	Correlation coefficient between the two random variables of load and resistance
$\boldsymbol{\alpha_i}$	Sensitivity coefficient
β	Reliability index
$\boldsymbol{\varepsilon}$	Convergence of the reliability index
ξ	Internal angle of friction, Drucker-Prager (°)
$\boldsymbol{\mu}$	Mean (in normal distribution)
$\boldsymbol{\mu'}$	Mean (in lognormal distribution)
$\boldsymbol{\mu_g}$	Mean of the limit state function
$\boldsymbol{\mu_Q}$	Mean load function
$\boldsymbol{\mu_R}$	Mean resistance function
$\boldsymbol{\mu_{x_i}}$	Mean value of the random variable x_i

References

Agricultural Statistics. (2002-2017). Office of Statistics and Information Technology. Tehran. *Ministry of Jihad Agriculture, Deputy of Planning and Economy, Office of Statistics and Information Technolog*y. (In Farsi).

Abo Al-kheer, A., El-Hami. A., Kharmanda, M. G., Mouazen, A. M. (2011). Reliability-based design for soil tillage machines. *Journal of Terramechanics*, 48 (1), 57–64.

Dudzik, A., Potrzeszcz-Sut, B. (2019). The structural reliability analysis using explicit neural state functions. *MATEC Web of Conferences 262*, https://doi.org/10.1051/matecconf/201926210002.

Elegbede, C. (2005). Structural reliability assessment based on particles swarm optimization. *Journal of Structural Safety*, Vol. 27, No. 2, pp. 171–186.

Ghohani Arab, H., Ghasemi M. R. The proposed new and low-cost method in calculating the probability of failure of problems based on the Monte Carlo method. *Journal of Modeling in Engineering*. Sixteenth year, No. 54, autumn 2018. (In Farsi).

Godwin, R. J., O'Dogherty, M. J., Saunders, C., & Balafoutis, A. T. (2007). A force prediction model for moldboard plows incorporating the effects of soil characteristic properties, plow geometric factors and plowing speed. *Journal of Biosystems Engineering*, 97 (1), 117-129.

Hasofer, A.M. and Lind, N.C. (1974). Exact and invariant second moment code format. *Journal of the Engineering Mechanics Division*, Vol. 111, No. 21, pp. 111-121.

Kaveh, A., Kalat jari, V. R. (1994). Theory of reliability and its application in structural engineering. *Iran University of Science and Technology Publications* (.In Farsi).

Keshtegar, B., Mirei, M., Shabakhti, N. (2011). Calculation of reliability index based on nonlinear conjugate gradient method. *6th National Congress of Civil Engineering*, 26 and 27 April, Semnan University, Semnan. Iran. (In Farsi).

Keshtegar, B., Miri, M. (2014). Introducing Conjugate gradient optimization for modified HL-RF method. *Journal of Engineering Computations*, Vol. 31, No. 4, pp. 775-790.

Keshtegar, B. (2018). Improvement of Stability Transformation Method for First Order Reliability Analysis. *Journal of Applied and Computational Sciences in Mechanics*, 28 (2), 143-152. (In Farsi).

Keshtegar, B. (2018). First-order reliability analysis of structures using the Harmonized Search optimization method. *Journal of Modeling in Engineering*, 51 (15), 15-27. (In Farsi).

Kharmnda, G., Ibrahim, M. H., Abo Al-Kheer, A., Guerin, F., El-Hami, A. (2014). Reliability-based design optimization of shank chisel plow using optimum safety factor strategy. *Journal of Computers and Electronics in Agriculture*, 109, 162-171.

Lee, J. O., Yang, Y. S. and Ruy, W. S. (2002). A comparative study on reliability-index and target-performance-based probabilistic structural design optimization. *Journal of Computers & structures*, 80 (3), pp 257-269.

Miar Naeimi, F., Azizyan, G. H., Akbari, G. H. (2016). Performance Evaluation of Monte Carlo Simulation and FORM Method to Calculate Probability of Failure for Concrete Gravity Dams in Sliding Failure Mode under Static Loading. *Modares Civil Engineering Journal (M.C.E.J)*, 16 (3), 227-240. (In Farsi).

Moghimi, H. (2020). Reliability Analysis of Stream Network Density Changes in Urmia Lake Catchment Area Using FORM Probabilistic Method. *Iran-Water Resources Research*, 16 (3), 188-197. (In Farsi).

Mojahed, M. M., Ahmadi Nedushan, B. (2013). Reliability analysis of steel frames based on advanced methods of Monte Carlo. *7th National Congress of Civil Engineering. Shahid Nikbakht Faculty of Engineering*. 17 and 18 May. Sistan and Baluchestan University. Zahedan. (In Farsi).

Nazemosadat, S. M. R., Ghanbarian, D., Naderi-Boldaji, M., Nematollahi, M. A. (2022). Structural Analysis of a Mounted Moldboard Plow using Finite Element Simulation Method. *Spanish Journal of Agricultural Research.* (Accepted for Publication). https://doi.org/10.5424/sjar/2022202-18157.

Nowak, A.S., Collins, K.R. (2000). *Reliability of Structures.* Mc Graw-Hill, New York.

Nowak, A.S., Collins, K.R. (2012). *Reliability of Structures.* Second Edition. CRC Press, New York.

Saidi-Mehrabad, M., Fazlollahtabar, H. (2016). Monte Carlo Simulation to Compare Markovian and Neural Network Models for Reliability Assessment in Multiple AGV Manufacturing System. *Journal of Optimization in Industrial Engineering* 19, 75-85.

Shabakhti, N., Ghaffarpour Jahromi, S., Ahmadi, R. (2021). Reliability Analysis of Static Stability of Reinforced Soil Walls. *Journal of Civil Engineering Amirkabir*, 52 (10), 2451-2470. (In Farsi).

Shabakhti, N., Ghaffarpour Jahromi, S., Rahimi, R. (2021). Reliability Analysis of Piles under Lateral Load. *Journal of Marine Engineering*, 34 (7), 49-59. (In Farsi).

Sharifi, M., Yaghoubizadeh, M. (2015). Reliability modelling of the Redundancy Allocation Problem in the Series-parallel Systems and Determining the System Optimal Parameters. *Journal of Optimization in Industrial Engineering* 17, 67-77.

Shayanfar, M., Ghanooni Bagha, M., Jahani, E. (2015). Reliability Theory of Structures. *Iran University of Science and Technology Publications*. (In Farsi).

Sorensen. J. D. (2004). Structural Reliability Theory and Risk Analysis. *Institute of Building Technology and Structural Engineering Aalborg University*.

This article can be cited: Nazemosadat, S. M. R., Naderi-Boldaji, M., Ghanbarian, D., & Nematollahi, M. A. (2022). Reliability Analysis of a Mounted Moldboard Plow Bottom Standard using the FORM Method. *Journal of Optimization in Industrial Engineering*, *15*(2), 179-190. Doi: 10.22094/joie.2022.1932748.1868